DOI: 10.21062/mft.2022.064 http://www.journalmt.com

A Modified Thermal Model of Internal Grinding

Zhou Chang[1*] (0000-0002-2619-0290), Lai Hu[2] (0000-0002-7715-5612)
[1]School of mechanical and electrical engineering, Lanzhou Jiaotong University, Lanzhou, Gansu, P.R. China 730070 E-mail: starismyfriend@163.com
[2]State Key Laboratory for Manufacturing System Engineering, Xi'an Jiaotong University, Xi'an, Shaanxi, P.R. China, 710054

In the present study, an innovative method is proposed to improve the accuracy of thermal models of the grinding process. To this end, a set of orthogonal experiments are carried out to calculate heat flux using infrared temperature measurements. Then the convective heat transfer coefficient is modified based on the heat transfer and hydrodynamics theories. Finally, the modified heat flux and convective heat transfer coefficient are applied and a thermal model is established using ANSYS software. To verify the accuracy of the proposed model, a finite element grinding residual stress model based on the grinding heat and grinding force is established. By measuring the grinding residual stress and comparing it with the finite element residual stress model, the effectiveness of the grinding thermal model is indirectly verified. The obtained results demonstrate that the modified grinding thermal models are accurate and can be applied in engineering applications.

Keywords: Convective heat transfer, Heat distribution ratio, Grinding heat, Residual stress, Finite element method

1 Introduction

Grinding is an important machining process, which is widely used in precision machining. During a grinding process, significant heat is generated. On the other hand, high grinding temperatures may result in grinding burn. The grinding burn refers to the change of metallographic structure on the workpiece surface, which results in the formation of residual tensile stress and decreases the workpiece hardness. Studies show that the grinding temperature reduces the fatigue life of the workpiece. Therefore, it is of great significance to study the grinding heat and reduce the grinding temperature.

Reviewing the literature indicates that numerous analytical models have been proposed to study the surface grinding temperature. However, it is a challenge to establish an analytical model in complex grinding methods such as forming grinding. In order to resolve this problem, numerical methods, including the finite element method and finite difference method, have been applied to study the grinding temperature field model. In this regard, Guo and Malkins (C Guo, S Malkin, 1995) studied the grinding temperature using the finite difference method. Moreover, Shen (B Shen, AJ Shih, G Xiao, 2011) used the finite difference method to analyze the grinding temperature field. Then the established grinding thermal model was verified through experiments. Mahdi and Zhang (M Mahdi, L Zhang, 1995) used the finite element method to study the grinding temperature field and calculated the martensitic transformation depth of alloy steel. With the rapid development of the numerical method in the past few decades, the finite element method has been widely used to simulate the grinding temperature field.

When using the finite element method to study the grinding temperature field, some parameters should be given by experience. Accordingly, the grinding temperature field obtained from the finite element method is often not accurate enough. Aiming at resolving this problem, a modified grinding temperature field model is proposed in the present study. To this end, the grinding heat distribution ratio is revised using infrared thermal image experiments. Moreover, the convective heat transfer coefficient is revised based on the heat transfer theory, and a model is established to calculate the finite element grinding heat the residual stress. Finally, the residual stress is measured and verified using the finite element model. The proposed method is expected to improve the accuracy of the finite element thermal model and lay a foundation for practical engineering application.

2 Grinding test

The grinding experiment was carried out on a bearing raceway grinder (Company 3mk1420, China). The grinding wheel is made of corundum and the model is p80 × 10 × 20A80KV60. The grinding wheel is trimmed with a single-point diamond pen dresser, and the grinding fluid is an emulsion. Accordingly, the performance of the grinding wheel is consistent. The grinding workpiece is the outer ring of the heat-treated

angular contact ball bearing. The inner and outer diameters of the ring test piece are 98 mm and 110 mm, respectively. Moreover, the widths of the ring test piece and raceway are 20 mm and 7 mm, respectively. The material of the ferrule is bearing steel GCr15. Fig. 1 shows the configuration of the processing equipment.

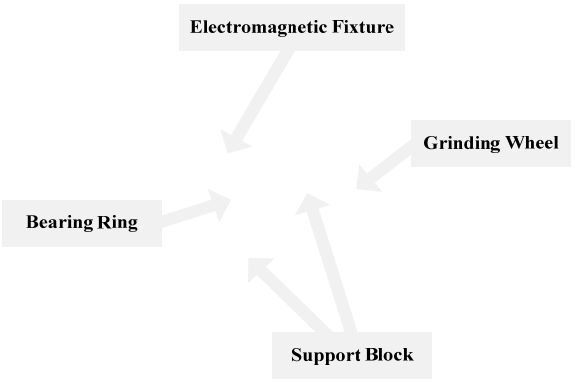

Fig. 1 *Configuration of the grinding equipment*

Generally, there are two ways to measure the grinding temperature: infrared and thermocouple. Infrared technology can be mainly divided into infrared thermal imager and infrared optical brazing technology. Infrared optical fiber and thermocouples are usually used to measure the temperature at a certain point in the grinding temperature field. In this method, it is necessary to punch holes in the workpiece to install infrared optical fibers and thermocouples. This method has been widely applied in surface grinding experiments.

In the grinding experiment of bearing outer ring raceway, the wall thickness of the ring is relatively thin. Accordingly, it is a challenge to drill the specimen and install a thermocouple or infrared optical fiber. The main objective of the present study is to use infrared thermal imager technology to measure the grinding temperature of the inner circle. The main advantage of this method is that the whole grinding temperature field is measured, and there is no need to drill holes in the workpiece. On the other hand, the main disadvantage of this method is that the measured temperature field is greatly affected by the environment. Because the grinding wheel blocks the grinding contact area during inner circle grinding, only the temperature field outside the contact area can be measured. Considering the influence of the grinding fluid on the measurement, the temperature field can be measured only during dry grinding. Consequently, the infrared thermal imager technology can only be used to measure the temperature field outside the grinding contact area during dry grinding. Then the temperature rise can be calculated, indicating the temperature field in the grinding contact area.

Tab. 1 *Elemental composition of bearing steel (GCr15)*

Element	C	Mn	Si	Cr	Mo
min. wt%	0.98	0.25	0.15	1.30	0
max. wt%	1.10	0.45	0.35	1.60	0.10

Tab. 2 *Performance parameters of GCr15 quenched material*

Material	Temperature (°C)	Density (kg/m3)	Modulus of elasticity (GPa)	Poisson's ratio	Hardness	Yield strength (MPa)
GCr15	20	7830	208.1	0.3	HRC62	1410

Studies show that the wheel speed, workpiece speed, and grinding depth are the three main factors affecting the grinding temperature rise in a dry grinding process. Accordingly, these parameters are considered to design measurement experiments of the L9 orthogonal table.

The measurement results obtained from the infrared thermal imager are shown in Fig.2.

The infrared temperature of the first group of parameters during dry grinding is selected as the calibration temperature, and the absolute value of the temperature difference between the other 8 groups of parameters and the first group is selected as the temperature rise.

Tab. 3 *Grinding orthogonal test table*

Test No.	Grinding wheel speed n_s (r.min^{-1})	Workpiece speed n_w (r.min^{-1})	Grinding depth a_p (μm)
1	5000	100	5
2	5000	150	10
3	5000	200	15
4	7000	100	10
5	7000	150	15
6(best)	7000	200	5
7	9000	100	15
8	9000	150	5
9(best)	9000	200	10

Fig. 2 *Infrared measurement of the grinding temperature field*

3 Correction of the workpiece heat flux experiment

In the present study, the grinding thermal model is established using the finite element method. In this model, heat flux is an important parameter, which directly affects the accuracy of the finite element thermal model. The total heat flux generated can be calculated from the following expression:

$$q_t = \frac{v_s F_t}{b l_g} \tag{1}$$

Where:

v_s …The linear speed of the grinding wheel,

F_n …The tangential grinding force,

b …The grinding width,

l_g …The length of the grinding contact area.

The tangential grinding force can be calculated from the following expressions [11]:

$$\begin{cases} F_n^{'} = 5.95 v_s^{-0.641} v_w^{0.255} a_p^{0.718} d_e^{0.282} \\ F_t^{'} = 5.05 v_s^{-0.848} v_w^{0.352} a_p^{0.705} d_e^{0.295} \end{cases} \tag{2}$$

where F_n and F_t denote the normal and tangential grinding force per unit width, respectively. Moreover, d_e is the equivalent grinding wheel diameter. In dry grinding, the heat flux entering the workpiece is as follows:

$$q_w = q_t \cdot \varepsilon = \varepsilon \frac{F_t \cdot v_s}{b \cdot l_g} \tag{3}$$

Where:

ε …The heat distribution ratio.

The temperature rise of the internal grinding surface can be obtained from the following expressions [11]:

$$\begin{aligned} T_{dry} &= \frac{2\alpha R_w}{\pi k v_w} \cdot \int_0^{\theta} q_w(r_w \theta_i) \cdot g(\theta_i) \mathrm{d}\theta_i \\ g(\theta_i) &= \exp[-R_w \sin(\varphi - \theta_i)] K_0[2R_w \sin(\frac{\varphi - \theta_i}{2})] \end{aligned} \tag{4}$$

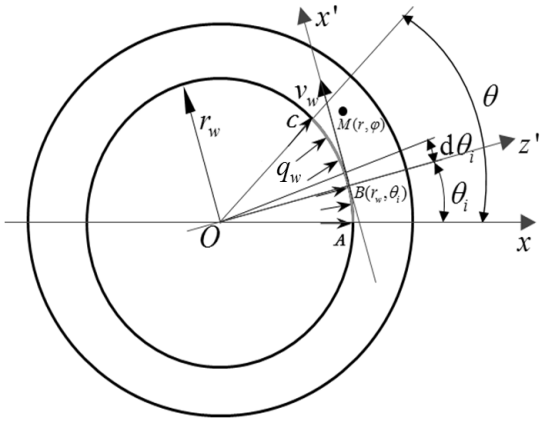

Fig. 3 ***C****oordinate system of heat source on the inner circle grinding surface*

Equations 4 and 5 indicate that the temperature rise is a function of the heat distribution ratio. When the other grinding parameters are determined, the heat entering the workpiece determines the temperature rise. In conventional finite element thermal models, the heat distribution ratio entering the workpiece mostly adopts experience or the value, which mostly varies in the range of 0.55 to 0.7. In the present study, the infrared temperature measurement experiment is used to modify the parameter of heat distribution ratio and establish the grinding heat model in accordance with the actual working conditions.

In the present study, an objective optimization function is established and the heat distribution ratio consistent with the real working condition is obtained in the form below:

$$F(\varepsilon) = (\Delta T_1 - \Delta T_1^{'})^2 + (\Delta T_2 - \Delta T_2^{'})^2 \cdots + (\Delta T_8 - \Delta T_8^{'})^2 \quad (5)$$

Where:

ε …The heat distribution ratio, the temperature rise simulated by the finite element method, and the experimental temperature rises, respectively.

When the minimum value is obtained, the optimal value of the parameter is obtained. Therefore, the problem of dry grinding heat with a modified heat distribution ratio can be transformed into the solution of the following equation:

$$\begin{cases} \min F(\varepsilon) \\ s.t. 0.55 \le \varepsilon \le 0.7 \end{cases} \quad (6)$$

When the heat distribution ratio is determined, the heat flux entering the workpiece can be calculated accurately.

4 Theoretical correction of the convective heat transfer coefficient

In the finite element simulation of the wet grinding process, it is an enormous challenge to determine the convective heat transfer coefficient. The parameters are mostly set by experience or the experimental results. In this regard, the theory of heat transfer and hydrodynamics have been used to deduce the calculation method of the convective heat transfer coefficient. To this end, a new method is proposed to calculate the convective heat transfer coefficient.

According to heat transfer theory, the Nusselt number can be expressed as follows:

$$N_u = \frac{h_f l_c}{k_f} = 0.664 \times \mathrm{Re}^{1/2}\,\mathrm{Pr}^{1/3} \quad (7)$$

Accordingly, the convective heat transfer coefficient can be written as follows:

$$h_f = 0.664 \cdot k_f \cdot \mathrm{Re}^{1/2}\,\mathrm{Pr}^{1/3} / l_c \quad (8)$$

$$\mathrm{Re} = \frac{\rho_f v_{av} l_c}{\mu_f} \qquad \mathrm{Pr} = \frac{\mu_f c_f}{k_f} \quad (9)$$

Where:

l_c …The actual contact arc length of the grinding area, which can be calculated using the following expression:

$$l_c = [R_r^2 8F_n^{'}(K_s + K_w)d_s + ad_s]^{0.5} \quad (10)$$

Combining Eqs. (8)-(10) yield the convective heat transfer coefficient.

In the present study, the two-dimensional steady-state navistokes equation is solved:

$$\frac{\partial^2 u}{\partial y^2} = \frac{1}{\mu_f}\frac{\partial p}{\partial x} \quad (11)$$

Eq. (11) is subjected to these boundary conditions: dP/dx = 0

Solution of Eq. (11) subjected to the boundary condition (xx) can be expressed in the form below:

$$u = \frac{1}{2\mu_f}\frac{\partial p}{\partial x}(y^2 - yH) + (v_s - v_w)\frac{y}{H} + v_w = (v_s - v_w)\frac{y}{H} + v_w \quad (12)$$

Accordingly, the average flow velocity in the section of grinding contact area is:

$$v_{av} = \frac{1}{A}\int_A u dA = (v_s + v_w)/2 \quad (13)$$

Finally, the convective heat transfer coefficient can be calculated as follows:

$$h_f = G\sqrt{\frac{(v_s + v_w)/2}{l_c}} \quad (14)$$

$$G = 0.664 \times \rho_f^{1/2} \times k_f^{2/3} \times c_f^{1/3} \times \mu_f^{-1/6} \quad (15)$$

The convective heat transfer coefficient is calculated by using 9 groups of data of orthogonal tests, and the convective heat transfer coefficient is between 30,000 and 50,000.

5 Finite element thermal model

In this article, the grinding heat of a 3D model is analyzed using ANSYS software. The calculated heat flux and the convective heat transfer coefficient are used to accurately establish the thermal model of the grinding temperature field.

The thermophysical parameters of the workpiece such as thermal conductivity, density, and specific heat depend on the temperature. These parameters are presented in Table 2.

Tab. 4 *Thermophysical parameters of hardened bearing steel GCr15*

Temperature (°C)	20	100	200	300	400	500
Thermal conductivity ($W/m^{\circ}C$)	43	40.35	39.95	37.97	36.39	34.41
density (kg/m^3)	7830	7806	7776	7744	7709	7672
heat scale ($J/kg^{\circ}C$)	480.1	513.2	540.8	579.4	618.1	673.2

To ensure the accuracy of the calculation, the mapping grid method is used to mesh the network and obtain a regular hexahedral grid.

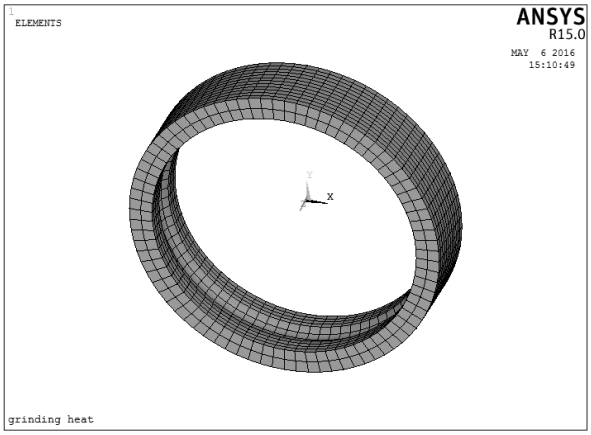

Fig. 4 *Meshed model*

Transient analysis is performed to obtain the grinding temperature field. During wet grinding, one end face of the workpiece is in contact with the electromagnetic centerless fixture, and there is grinding fluid on the other surfaces. Therefore, convective heat transfer is applied to the surface with a grinding fluid. Accordingly, surface thermal effect elements are considered in calculations.

The moving heat source is loaded on the ferrule raceway. To this end, a fixed heat source is loaded in one grinding area in a very short time, then another area with a fixed heat source is considered in the next period. Finally, the last result is considered the initial condition of this time.

Fig. 5 reveals that the maximum grinding temperature is 574 ℃. It is found that when the grinding temperature exceeds 400 ℃, the residual tensile stress occurs in bearing steel. Meanwhile, when the grinding temperature is lower than 400 ℃, residual compressive stress occurs in the grinding area. The grinding temperature is calculated using 9 groups of data in the orthogonal test, where the grinding temperature is between 300 and 500 degrees of centigrade.

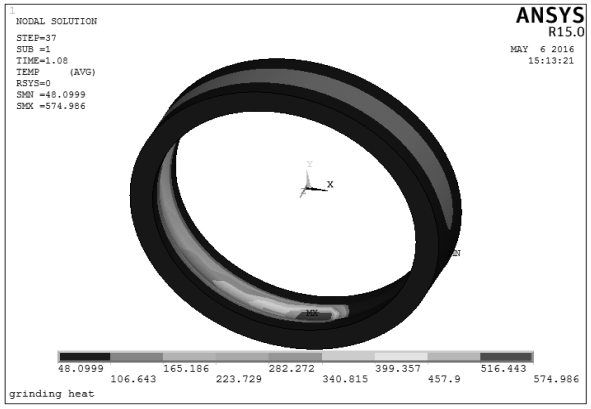

Fig. 5 *Temperature distribution of the workpiece*

6 Experimental verification

The residual stress is an important indicator of the surface integrity. In this paper, the residual stress was measured and recorded in detail using an X-350A X-ray diffractometer. Because the raceway width of the angular contact ball bearing (7014AC) was 7 mm, the width of the X-ray irradiation area had to be smaller. To ensure a high accuracy of the residual stress measurements, the smallest collimator was selected. The largest possible X-ray tube voltage and tube current were selected, as well as the longest counting time.

After grinding, the bearing ring was cut into three sections using a linear cutting machine, so it was convenient to measure the residual stress of the inner raceway using an X-ray diffractometer. Figure 2 shows a photograph of a specimen.

Generally, the residual stress of the raceway will be released when cutting the bearing ring into pieces. However, Yan et al. [19] used the finite element method to study the variation of the residual stress distribution in a thick aluminum plate after cutting. The results showed that the residual stress is lowest at the cutting edge. When measuring the residual stress at a certain distance from the cutting edge, and the distance is approximately equal to the thickness of the test specimen, the variation of the residual stress is small and can be ignored. Therefore, when using a proper cutting method and a proper measurement method, the residual stress of the bearing raceway can be accurately measured.

In order to ensure a high accuracy of the measurements, the measurements had to be performed normal to the test point vertical. A small ball was used as attachment, and the ball diameter was smaller than the raceway width. A small ball was used to determine the lowest point of the bearing raceway of the piece, and this stationary point was used as the measurement point for the X-350A X-ray diffractometer. The measurement point was far away from the cutting edge, and the distance was far greater than the thickness of the bearing ring, so the measured residual stress of the ring was considered to be accurate.

The residual stress of the raceway surface is in a biaxial stress state. In this study, we measured the axial residual stress and the circumferential residual stress of each bearing raceway. A total of nine groups of orthogonal arrays were designed, with five rings in each group which were ground according to the grinding parameters of each group. Each ring was cut into three pieces. First, the residual stress of each section was measured, and then the average residual stress of each ring was calculated. Next, the average residual stress of the five rings in each group was calculated. The average residual stress of the rings is presented as the final measurement results.

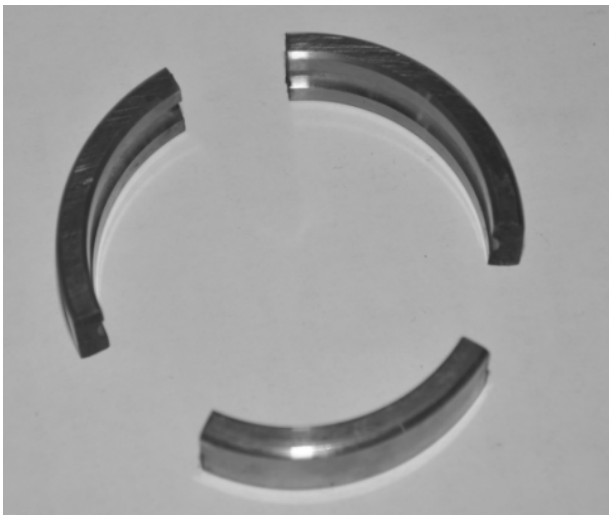

Fig. 6 *The bearing outer ring samples which are cut*

In order to verify the performed simulations, the residual stress of the bearing grinding raceway is compared with the calculated values. Because the burn is strictly controlled during grinding, the influence of the phase transformation is ignored. In other words, the effects of grinding heat and grinding force on the residual stress of the bearing raceway are considered in the calculations.

The temperature field is analyzed using the temperature unit (solid90). When the grinding temperature is obtained, the temperature unit is transformed into the structural unit (solid185) to couple the field analysis. The calculation results of the grinding temperature field are introduced first, then the grinding load is applied and finally, the grinding residual stress is obtained. The loading method is similar to that of the grinding heat source. The movement process of grinding force along the workpiece surface is discretized. A uniformly distributed grinding force is loaded in a grinding area in a very short time and moved to another area in the next period to load the uniformly distributed grinding force, and the last result is taken as the initial condition of this time.

After grinding, the test specimen is cut into small sections, and the residual stress of the small section is measured using an X-ray diffractometer (Company x350a, Country). After the ferrule is untied, the residual stress will be released to a certain extent. To ensure measurement accuracy, it is necessary to adopt appropriate measurement methods. When the distance between the measuring position and the cutting edge is much greater than the wall thickness of the ferrule, the measurement result is more accurate.

Fig. 6 reveals that the distributions of experimental and calculated circumferential residual stress are relatively consistent. The measured value of circumferential residual stress is about 30% larger than the finite element simulation value. In this paper, the grinding force model used in finite element simulation is an analytical solution, which is more accurate. The thermal model of finite element simulation will bring some errors, so it leads to the error of the residual stress model. For the finite element thermal model, the error of 30% is acceptable.

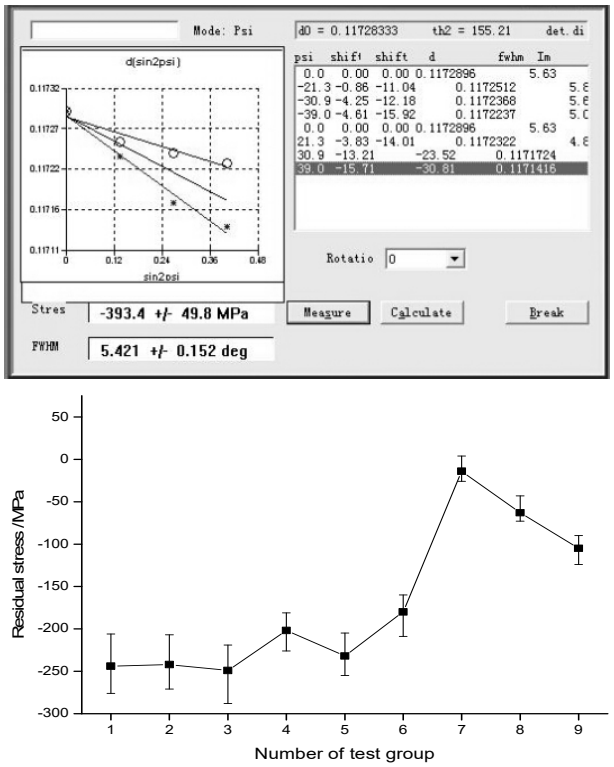

Fig. 7 *Comparison of circumferential residual stress simulation experiment*

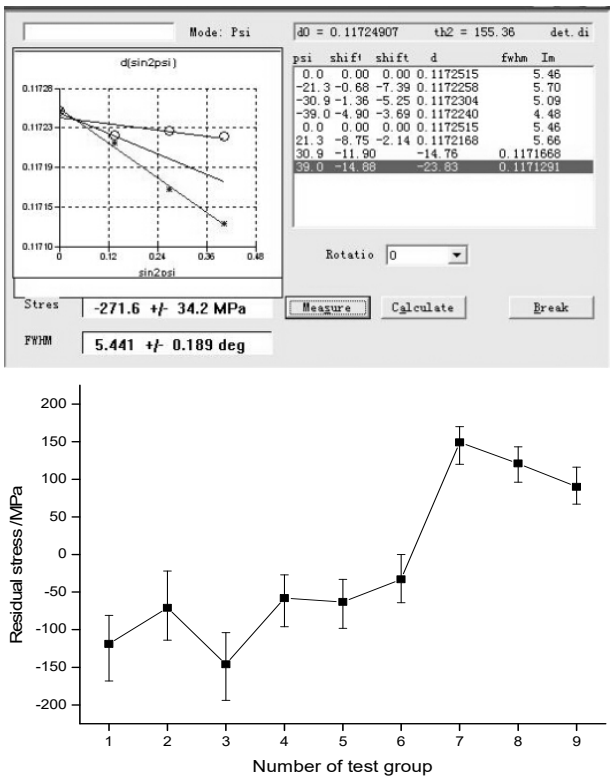

Fig. 8 *Distribution of the axial residual stress*

Fig. 7 indicates that the distributions of experimental and calculated circumferential residual stress are consistent, and the measured value of the circumferential residual stress is about 30% greater than the finite element simulation value. Because the axial direction is perpendicular to the grinding direction, the contrast fluctuation between the measured and simulated values of axial residual stress is more obvious. The simulation value of axial residual stress is compared with the experimental value, which also verifies the correctness of the finite element thermal model, and the error is about 30%.

Fig. 9 *Test bench to measure the residual stress*

7 Conclusion

In the present study, a modified finite element grinding thermal model is proposed. The obtained results reveal that the accuracy of the thermal model is 70%.

The orthogonal temperature measurement experiment is carried out to obtain the temperature field outside the contact area of dry grinding using an infrared thermal imager. The heat distribution ratio is 0.66, and the heat flux entering the workpiece is determined.

Based on heat transfer and hydrodynamics, a method is proposed to calculate the convective heat transfer coefficient in a grinding process. The convective heat transfer coefficient of 9 grinding orthogonal tests is 30,000-50,000.

Using the modified heat flux and convective heat transfer coefficient, the finite element model of grinding residual stress is established. Compared with the test results of residual stress, the effectiveness of the grinding thermal model is verified.

Funding

This research was funded by the Gansu Provincial Natural Science Foundation, grant number 21JR11RA066; the Natural Science Foundation of Lanzhou Jiaotong University, grant number 2021017.

Competing interests

The authors declare that they have no competing financial interests.

Data Availability Statement

The raw/processed data required to reproduce these findings cannot be shared at this time as the data also forms part of an ongoing study.

Acknowledgments

The authors wish to acknowledge Dr Chen, professor of Xi'an Jiaotong University, for his help in interpreting the significance of the results of this study.

Reference

[1] S. MALKIN, C. GUO (2007) Thermal Analysis of Grinding. *CIRP Annals - Manufacturing Technology* 56(2):760-782

[2] W.B. ROWE (2001) Thermal analysis of high efficiency deep grinding. *International Journal of Machine Tools & Manufacture* 41(1):1-19

[3] D.J. STEPHENSON, T. JIN, J. CORBETT (2002) High Efficiency Deep Grinding of a Low Alloy Steel with Plated CBN Wheels. *CIRP Annals - Manufacturing Technology* 51(1):241-244

[4] C. GUO, S. MALKIN (1995) Analysis of Transient Temperatures in Grinding. *Journal of Engineering for Industry* 117(4):571-577

[5] B. SHEN, A.J. SHIH, G. XIAO (2011) A Heat Transfer Model Based on Finite Difference Method for Grinding. *Journal of Manufacturing Science & Engineering* 133(3):255-267

[6] M. MAHDI, L. ZHANG (1995) The finite element thermal analysis of grinding processes by ADINA. *Computers & Structures* 56(2–3):313-320

[7] M.P.L. PARENTE, R.M.N. JORGE, A.A. VIEIRA, A.M. BAPTISTA (2012) Experimental and numerical study of the temperature field during creep feed grinding. *International Journal of Advanced Manufacturing Technology* 61(61):127-134

[8] A.M.O. MOHAMED, A. WARKENTIN, R. BAUER (2012) Variable heat flux in numerical simulation of grinding temperatures. *International Journal of Advanced Manufacturing Technology* 63(5-8):549-554

[9] D. ANDERSON, A. WARKENTIN, R. BAUER (2008) Experimental validation of numerical thermal models for dry grinding.

Journal of Materials Processing Technology 204(1–3):269-278

[10] D. ANDERSON, A. WARKENTIN, R. BAUER (2008) Comparison of numerically and analytically predicted contact temperatures in shallow and deep dry grinding with infrared measurements. *International Journal of Machine Tools & Manufacture* 48(3–4):320-328

[11] TOMAS BAKSA, PAVEL ADAMEK, ONDREJ HRONEK, MIROSLAV ZETEK (2019) Degradation of a Grinding Wheel when Grinding Cermet Materials and Its Influence on the Grinding Process. *Manufacturing Technology* 19(5):855-859

[12] DANA STANCEKOVA, ANNA RUDAWSKA, MIROSLAV NESLUŠAN, JOZEF MRÁZIK, MIROSLAV JANOTA (2019) The Implementations of Suitable Cutting Parameters by Grinding of Titanium VT9 with Impact on Surface Integrity. *Manufacturing Technology* 19(1):9-13

[13] WU HUAI-CHAO, ZHAO LI-MEI, YAN WEN-MENG, XU LEI (2019) Design and Dynamic Performance Study on Hydrostatic Lubrication System of High-speed Precision Roller Grinding Head. *Manufacturing Technology*, 19(6):959-965